REMOTE SENSING OF ENVIRONMENT 15:47–61 (1984)

Ground Level Solar Energy Estimates Using Geostationary Operational Environmental Satellite Measurements and Realistic Model Atmospheres

PAUL HALPERN

IBM Corporation, Palo Alto Scientific Center, Palo Alto, California 94304

A radiative transfer model and measured radiance values from the Geostationary Operational Environmental Satellite are used to obtain estimates of ground level solar insolation. These are compared to surface observed data monitored in Northern California. The estimates of solar insolation are obtained by using pixel data from a Geostationary Operational Environmental Satellite, in conjunction with ground reflectivity and zenith angle of the sun to choose an appropriate atmospheric model. The sophisticated radiative transfer model is then used to obtain the ground level estimate of insolation. The time integrated GOES-model estimated surface insolation values are within 3% of the measured data during a 3-day test period.

Introduction

Several early studies by Hanson (1971) and Vonder Haar and Ellis (1975) dealt with calculating monthly average surface insolation using ground measurements of reflectivity made by a polar orbiting satellite. However, these studies were not able to account for the daily variation in solar radiation values due to the limited set of observations made by this satellite over the study area. The capability to obtain quasicontinuous data for both the infrared and visible region of the solar-spectrum was accomplished with the launching of the Geostationary Operational Environmental Satellite (GOES). The GOES spacecraft, which orbits at approximately 36,000 km, spins about an axis oriented nearly parallel to the Earth's spin axis. The capacity of the GOES sensors to scan the same area in a quasi-continuous manner makes it possible to obtain transmission of reflected radiance measurements from the earth–atmosphere system every 30 min. Using GOES infrared measurements, Chen et al. (1979) obtained infrared night time surface temperature patterns near Lake Okeuchabye, Florida. Local hourly temperature patterns were found to be functions of soil types, soil depths and drainage. Tarpley (1979) used the GOES visible digital data to estimate solar radiation incident at the earth's surface. The GOES visible data are in the form of count values which are a measure of relative radiance from the earth–atmosphere system. Tarpley determined this radiance as a function of local zenith angle and azimuth angle between sun and satellite by evaluating a set of regression coefficients. These coefficients are associated with terms describing physical interactions which affect the beam of radiation as it traverses the atmosphere. The model accounted for absorption due to water vapor and scattering due to air molecules. Since GOES makes repeated observations in the visible spec-

52 Vanderbilt Ave., New York, NY 10017

0034-4257/84/$3.00

trum during the day, Tarpley obtained both hourly values of solar radiation and a daily integrated value. Gautier et al. (1980) used a simple physical model of the earth–atmosphere system and data obtained from the GOES visible sensor to calculate the insolation at ground level. The solar radiation incident at the earth's surface under clear sky conditions was made a function of the albedo, the reflection of both the direct and diffuse radiation beam from the earth atmospheric system and absorption by water vapor. The albedo is the ratio of the amount of radiation reflected by a body to the amount incident upon it. An advantage of using a physical rather than a statistical model is that the physical processes are modeled using parameters which can be measured directly. Thus the model can be tuned using these measured quantities.

The motivation for this investigation is the importance of estimating ground level insolation for agriculturally related activities including crop management, water budget analysis, and crop growth and yield modeling. Insolation values are also significant input parameters to plant physiological and soil moisture studies. A detailed climatological survey of surface insolation is also critical for locating potential sites for solar energy collection. In this current study, radiance data measured by GOES are converted to upward directed radiative flux values. These are matched to calculated fluxes obtained from a sophisticated radiative transfer model using several realistic model atmospheres. The benefit of this approach is that it incorporates the effect of multiple scattering, which can significantly affect the magnitude of the calculated flux. Furthermore, a feature of the transfer model is that it can be used to spectrally integrate wavelength dependent fluxes. Specifically when matching GOES measured flux and simulated flux, the transfer model permits a wavelength integration of the simulated flux over the spectral region in which GOES makes observations. From an operational point of view the use of the transfer model permits a precalculation of the simulated fluxes which are stored and accessed as a simple table look up. Additional atmospheric models can be added as desired to build a library of atmospheric models.

The radiative transfer model we choose is that developed by Dave and Braslau (1975). They have developed a basic set of atmospheric models which we used in conjunction with the GOES data. This set of model atmospheres is not potentially the optimum set with respect to matching the exact conditions under which the surface observations were taken. In particular, it is well established that a major atmospheric parameter which affects the incoming solar flux is the amount and type of cloud cover present. Such information would ideally be obtained from a coordinated set of surface observations. However, the surface observations used in this study were collected for an independent study in order to provide data for testing theories of simultaneous flow of heat and moisture in soil (Reginato et al., 1981). In particular, no aerosol data was collected at the test site. Thus there was no overall experimental design so that data gathered would provide input to a complex radiative transfer model. Nonetheless, we choose to use the model and observational data which, while a marriage of convenience, served both to initially test our hypothesis and to stimulate further model and observational data investigations.

Radiative Transfer Models

The extinction of radiation both from the direct and diffuse beam as it passes through the earth's atmosphere is caused by three processes:

1. Scattering by air molecules.
2. Scattering and absorption by aerosols (e.g., dust).
3. Gaseous absorption (e.g., water vapor).

Previously cited studies used GOES data in conjunction with model atmospheres that did not simulate the combined effect of absorption and multiple scattering by atmospheric aerosols. The scattering by aerosols can be a major contribution to the scattered skylight which makes up the diffuse beam. The significance of the radiation absorbed and scattered by aerosols was evaluated by radiative transfer calculations made by Dave and Braslau (1975). They developed a method for solving the radiative-transfer equation which considered all orders of scattering as well as absorption by aerosols. This model is unique in that the solar spectrum is divided into 83 wavelengths permitting a meaningful simulation of absorption by ozone, water vapor, carbon dioxide, and oxygen. The special features of the method also allow the radiative fluxes emerging from a one-dimensional modeled cloud to be computed with very high accuracies. Their simulation calculations for clear sky conditions showed that, relatively speaking, increasing the amount of aerosol has a greater effect on the energy absorbed within the earth–atmosphere system than the albedo of the earth's surface unless the aerosol is nonabsorbing. Halpern and Coulson (1978), in additional modeling calculations, showed that presence of an absorbing aerosol in high concentrations, such as in and around atmospheres of major urban areas, can significantly reduce solar radiation at the earth's surface by an order of 10–20%. A number of observational studies have also verified these findings (e.g., Peterson and Flowers, 1974).

For this study we use the radiative transfer model of Dave and Braslau (1975). The basic model atmosphere contains spherical particles with gaseous absorption due to ozone and water vapor specified in 50 layers from the surface (0 km) to the top of the atmosphere (50 km). The solar spectrum (0.285–2.5 μm) is divided into 83 wavelength intervals with appropriate functions representing scattering and absorption of gases, aerosol, and liquid water drops assigned to each.

The cloud layer modeled in the C1-ST and D1-ST atmosphere has the properties of an isolated cloud layer of water drops of refractive index $m = 1.34 - 0.0i$. The size distribution is that of cloud model C1 described by Deirmendjian (1969). The cloud's optical depth is such that the atmospheric spherical albedo is comparable to the observed albedo of the Earth's disc when illuminated by direct sunlight. The cloud model has an optical depth of 3.35 at a wavelength of 0.555 μm over the spectral range 0.255–2.5 μm. The cloud contains 2.05×10^6 average drops in a square centimeter column. The liquid water content is 0.0128 g^{-3}. The size distribution of the water drops is given by $n(r) = 2.373r^6 \exp(-1.5r)$, where $n(r)$ is the number of drops per unit volume, per unit interval of the radius at the radius r. The lower and upper cutoff for r is at 2 μm and 11 μm, respectively. The variations of volume scattering coefficient as a

function of wavelength and plane albedo as a function of scattering optical thickness are given by Dave and Braslau (1975). A drawback of this cloud model is that the optical thickness (0.555 nm) could be considered insufficient to represent some average cloud.

The model atmosphere is one representing midlatitude summer conditions given by McClatchey et al. (1970). Figure 1 shows the variations of ozone and water drops and aerosols as a function of height. The model makes use of the modified gamma distribution given by Deirmendjian (1969) to represent the size distribution. Table 1 shows the characteristics of the eight model atmospheres considered initially in this study. The solution of the radiative transfer equation for each model is expressed in terms of the energy passing through a unit area per unit time, i.e., the flux. For each model, tables of direct and diffuse flux for the 83 wavelength intervals were created. The flux values are not only functions of wavelength (λ) but also of zenith angle of the sun (θ_0), ground reflectivity (R), and height in the atmosphere (h). The flux values were computed for nine zenith angles of the sun, and 18 values of ground reflectivity. Since the major interest in this study is the spectrally integrated flux, the wavelength dependent fluxes are integrated over the 83 wavelength intervals. The spectrally integrated flux is given by

$$F(h,\theta_0,R)=\sum_{\lambda=0.285}^{\lambda=2.5} F(h,\lambda,\theta_0,R)\Delta\lambda. \tag{1}$$

where $\Delta\lambda$ is the wavelength interval. However, for a given distribution of radiation incident at the top of the atmosphere, we require the modeled flux at $h = 50$ km to be integrated over the spectral interval for which the GOES sensors

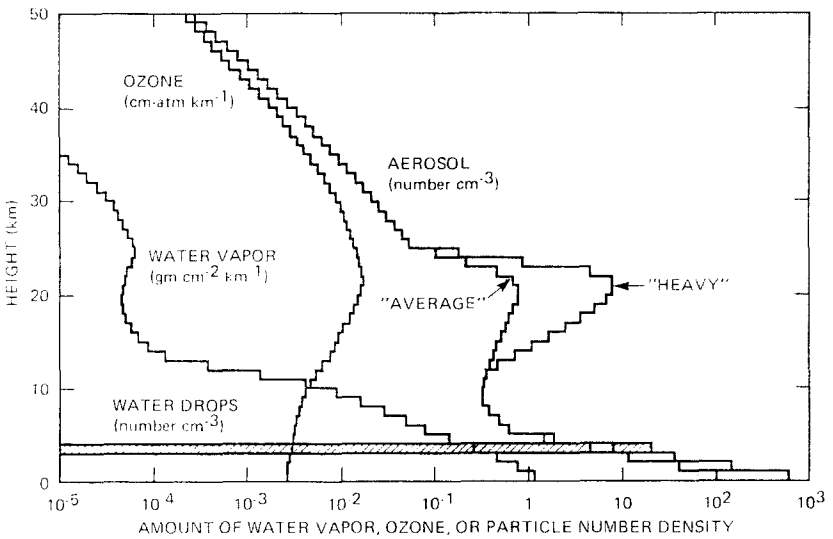

FIGURE 1. Variations of the water vapor; ozone aerosol and water drop number density as a function of height for model atmosphere.

TABLE 1 Atmospheric Models

Model	Gaseous Absorption	Aerosols	
		Height Distribution	Refractive Index
A	no	no	—
B	yes	no	—
C	yes	average	1.5–0.0i
D	yes	heavy	1.5–0.0i
C1	yes	average	1.5–0.01i
D1	yes	heavy	1.5–0.01i
C1-ST	yes	average	1.5–0.01i
D1-ST	yes	heavy	1.5–0.01i

measure visible radiation as shown in Fig. 2. This is comparable to 18 wavelength intervals in the modeled solar spectrum. Thus, an additional integration of the wavelength-dependent modeled fluxes over this spectral range was obtained. However, this integration is modified by the wavelength response of the visible sensors on GOES.

Processing and Analyzing GOES Data

There is an array of eight sensors which measure visible radiation on GOES. The image in the east–west direction is built by the sensors scanning with the spin of the space craft. The north–south scanning is accomplished by the sweep of the eight sensor array. The image recovered is

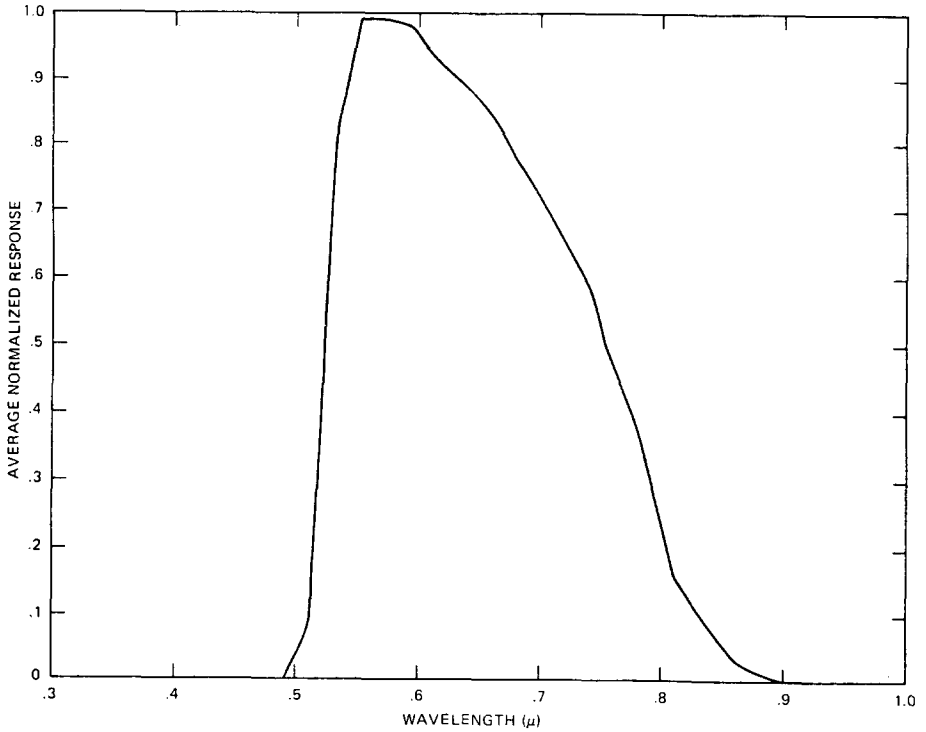

FIGURE 2. Averaged normalized response for the GOES Visible and Infrared Spin Scan Radiometer System (VISSR) sensor.

a superposition of these eight sensors. It is the practice of the National Environmental Satellite Service[1] to apply a transformation to the raw data for the purpose of reducing stripes which arise from differences among the detectors. The correction is derived statistically by constraining the digital signals of each detector to agree with an average response of all detectors in other parts of the image which have broad areas of uniform reflectance. The averaged normalized spectral response for all eight detectors is shown in Fig. 2.

The 1-km, high-resolution GOES images contain data from each of the eight sensors while the lower resolution 8-km data are an average over the eight sensors. Norton et al. (1980) point out that the image is recovered via a superposition of the several fields of view of each of the sensors. No further correction was made in our study and the count values are used as recorded on the data tapes. The data for the individual detectors were supplied by Comeyne (1980).

In order to determine the appropriate model atmosphere for obtaining the surface flux, it is necessary to determine the model values at 50 km which best approximate the GOES observed flux. To accomplish this, the model flux (at 50 km) must have the same spectral window as that of the GOES visible sensor. The spectrally integrated upward simulated fluxes at 50 km for the GOES spectral band is given by

$$F_S^{\uparrow}(50, \theta_0, R) = \sum_{\lambda = 0.40\,\mu}^{\lambda = 1.0\,\mu} \alpha(\Delta\lambda) F(50, \lambda, \theta_0, R) \Delta\lambda, \tag{2}$$

where $\alpha(\Delta\lambda)$ is the average normalized response for the spectral band interval $\Delta\lambda$ (Fig. 2).

The visible data measured by the sensors are in the form of 6-bit count values. The minimum value is the signal received from a black surface, and the maximum value is the signal received from a surface of 100% reflectance. The surface is also assumed to reflect radiation incident on it equally in all directions. This type of surface is called a Lambert surface. The conversion from count values to flux values is not well established. Gautier et al. (1980) used a calibration derived by Norton et al. (1980). In this study we choose a calibration method based on the observations of the GOES sensors from cloud tops. The energy per unit time coming from a specific direction θ_0 and passing through a unit area perpendicular to that direction is called the intensity. When the intensity is assumed to be uniform in all directions (isotropic), the flux can be expressed as

$$F(h) = \pi I(h). \tag{3}$$

It has been pointed out by Davis and Cox (1982) that reflected radiances will approach isotropic state only under a few restricted conditions such as over desert areas and at zenith angles less than 30°. At the larger zenith angles occurring during early morning hours and late in the afternoon when the anisotropy is at its maximum, the radiative intensity is at its minimum. Thus, for calculating daily integrated flux values the anisotropy effect should be minimized. The reflected flux from the top of a thick cloud at the top of the atmosphere $F(h, \theta_0)$ is given by

$$F(h, \theta_0) = \beta I_0 \cos\theta_0, \tag{4}$$

[1]Now called National Environmental Satellite Data and Information Service (NESDIS).

where I_0 is the intensity incident at the top of the atmosphere and β is the reflectivity of the cloud top. It is assumed that the cloud acts as a Lambert surface and attenuation suffered by the intensity between the top of the cloud and the top of the atmosphere is small. Investigations such as by Curran and Wu (1982) have attempted to determine radiance reflectance characteristics from cloud tops containing supercooled liquid water droplets. Comenye (1980) has indicated that for opaque clouds β as first approximation has a value of 0.85. Using reflected radiance values obtained from GOES observations of an intense Pacific hurricane and Eq. (4), a one point conversion curve for the visible sensor was obtained. Equation (5) shows the count to flux conversion curve as given by Norton et al. (1980):

$$\mathrm{NI} = (\mathrm{CV}/63)^2, \qquad (5)$$

where NI is the normalized reflected intensity and CV is the count value.

Using Eqs. (3) and (5), the values from individual pixels are converted to upward flux values measured by GOES $F_G^{\uparrow}(H, \theta_0, R)$, where H is the height of the GOES satellite. Under clear sky conditions, the library of atmospheric models is searched for the best matching upward simulated flux value $F_S^{\uparrow}(50, \theta_0, R)$, for the given zenith angle of the sun and ground reflectivity. Using the chosen model, the corresponding downward ground level flux $F_S^{\downarrow}(0, \theta_0, R)$ is obtained.

Under cloudy sky conditions, the sky cover in tenths as reported by ground based observations is used as an additional input parameter. The GOES data recorded under partially cloudy conditions necessitates a decision as to whether the pixel value represents a cloud or no cloud region. In previous studies, pixels were assigned a threshold value. Those pixels having a value less than this value were assumed to be cloud free, while those having a value greater than the threshold were assumed to be a cloud pixel. In the present study, the $F_G^{\uparrow}(H, \theta_0, R)$ value is compared to both cloud and no-cloud $F_S^{\uparrow}(50, \theta_0, R)$ values and the atmosphere model is chosen which best fit $F_G^{\uparrow}(H, \theta_0, R)$. In all the cloudy cases studied, the atmospheric Model C1-ST was the best fit model. As a first approximation to the cases where there is less than total sky cover, a weighted average is computed to obtain the surface flux. This is accomplished by weighting the $F_S^{\downarrow}(0, \theta_0, R)$ value for both the cloudy C1-ST model and the corresponding no-cloud C1 model by the fraction of sky cover and the fraction of clear sky, respectively.

Discussion of Results

Surface measured data

Total incoming solar flux was obtained at a specially instrumented site west of Sacramento, California (38°49′N, 121°59′W). The experimental site area is approximately 2.6 km^2. It is predominantly flat, and during the 1977–1978 crop growing season it was planted with barley. From the archived data set, ground level incoming solar flux for a 3-day period 7–9 April 1978 was compared to GOES estimated fluxes. This particular period was chosen because the atmospheric conditions with respect to the cloud amount varied from total skycover to clear sky conditions. In addition, the period was limited to 3 days because the volume of

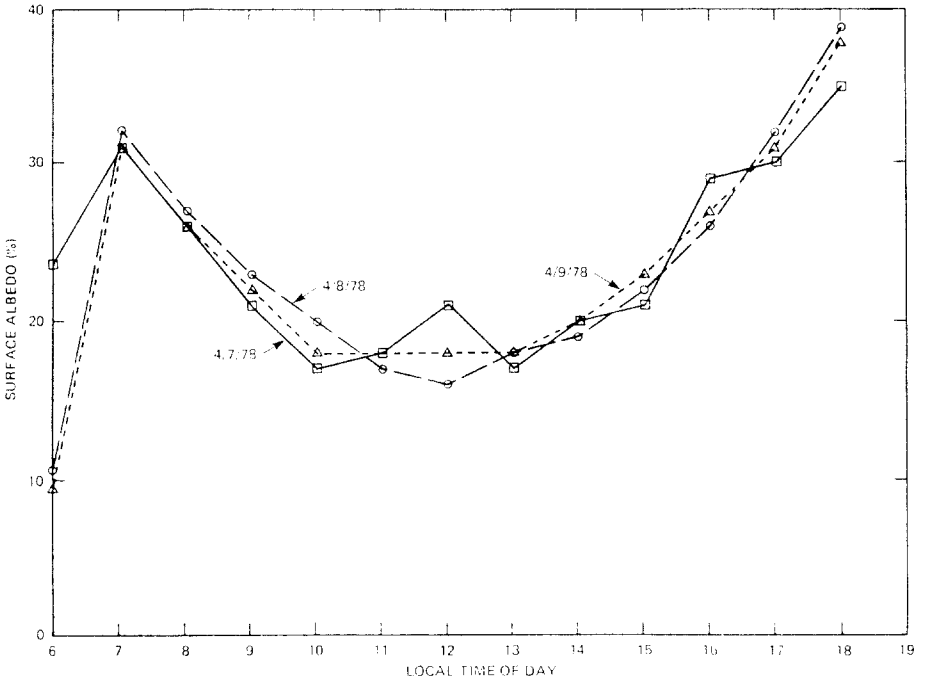

FIGURE 3. Representative surface albedo measurements as a function of local time for 7–9 April 1978.

GOES data required for a complete study of the data set would have been prohibitive. A detailed discussion and analysis of the measurement program is given by Reginato et al. (1981).

The GOES modeling calculations currently require estimates of the ground reflectivity. The variation of the ratio of the reflected to total observed flux (albedo), as a function of the time of day is presented in Fig. 3. These data and the flux data were recorded as averages taken over the first 20 min of the hour.

There were two locations within the test site where total incoming solar flux was measured. Since variations in readings between these monitoring sites were essentially subpixel in nature, spatially averaged flux values were computed. Figure 4 shows the variation of incoming solar flux as a function of the time of day. The large variations in the flux observed on 7 April 1978 was due to the presence of clouds which severely attenuated the insolation reaching the ground. During the subsequent 2 days which were relatively cloud-free, the magnitude of the flux increased, and its time rate of change was considerably smoother.

Comparison with surface data

The resolution of the visible sensors at the satellite nadir point is 0.9 km. This value deteriorates in the northern latitudes to a pixel resolution of the order of 2–3 km. The orbit and attitude information received from the space craft permit a conversion from latitude and longitude input to pixel and scan line output. However, the accuracy of this conversion is only to one or two pixels. Therefore, the data values were averaged over a 2×2 pixel array. This averaged value was con-

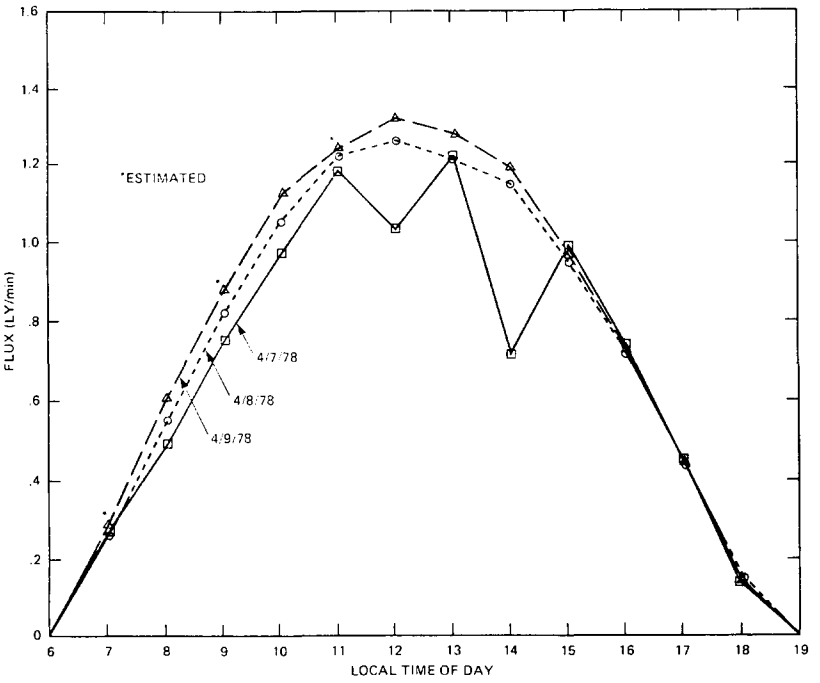

FIGURE 4. Spatially averaged variation of measured surface incoming solar flux as a function of local time for 7–9 April 1978.

verted to an estimate for the upward flux $[F_G^{\uparrow}(H, \theta_0, R)]$ assuming an isotropic intensity distribution. Both the GOES and model estimates used ground albedo values recorded at the test site (Fig. 3).

The flux data from the two locations monitoring total incoming flux were spatially averaged and compared to the simulated fluxes. An integrated flux value for the total time period was also obtained for the series of 20-min averaging periods using the trapezoidal rule. On the first day of the test period, 7 April 1978, the cloud cover varied from 10 tenths to clear sky. On this day, a weighted average of Model Cl-ST and Cl best matched the GOES flux. Table 2 shows the comparisons for 7 April 1978. With the exception of the 14 LST, the individual calculated fluxes are within 6% of the observed data. The estimated integrated value is within 2% of the observed flux. The effect of the clouds on the measured flux has been previously noted. The sharp reduction in flux at 14 LST is due to the presence of cloud variations which are on a time scale that the modeled GOES flux is unable to resolve. The large difference at 14 LST can be explained by these submodel variations due to cloud cover amount. Furthermore, the cloud cover amount changed most rapidly between 13 LST (8 tenths) and 15 LST (2 tenths). Thus the rapidly changing atmospheric conditions coincide with the time period for which the comparison between the satellite-model values and the surface observations are least favorable. These effects are somewhat masked when comparing the total integrated flux. Table 3 shows the comparison of the flux values for 8 April 1978. On this day there were no

TABLE 2 4/7/78: Comparison of Observed with Estimated Surface Flux (LY/min)

Hour	Surface Observation Locations 1	2	Avg	GOES Estimates	Ratio
08	0.468	0.517	0.49	0.43	0.88
09	0.769	0.729	0.75	0.75	1.00
10	1.056	0.884	0.97	0.97	1.00
11	1.173	1.194	1.18	1.17	0.99
12	0.943	1.111	1.03	1.09	1.06
13	1.238	1.209	1.22	1.18	0.97
14	0.720	0.728	0.72	1.07	1.49
15	1.001	0.982	0.99	0.96	0.97
16	0.704	0.775	0.74	0.70	0.95
Total integrated flux	150	150	150	153	1.02

TABLE 3 4/8/78: Comparison of Observed with Estimated Surface Flux (LY/min)

Hour	Surface Observation Locations 1	2	Avg	GOES Estimates	Ratio
08	0.531	0.561	0.55	0.54	0.98
09	0.809	0.838	0.82	0.87	1.06
10	1.052	1.050	1.05	1.10	1.05
11	1.223	1.212	1.22	1.24	1.02
12	1.302	1.212	1.26	1.30	1.03
13	1.225	1.185	1.21	1.27	1.05
14	1.148	1.158	1.15	1.15	1.00
15	0.950	0.944	0.95	0.93	0.98
Total integrated flux	150	148	149	153	1.03

clouds present and model D was the best fit model. The hourly estimates agree very well with the observed values. There is some overestimation of the flux for all the hours except early morning and late afternoon. This effect was also present in the integrated flux comparisons. The overestimate was also present on day 3 but to a lesser extent. Table 4 also shows the comparisons for 9 April 1978. Here the maximum GOES estimate is within 3% of the observed flux and the integrated flux values are within 2%. The simulations for this day were calculated using model Cl. There was a marked increase in both temperature and humidity on April 9 accompanied by a decrease in wind speed and a shift in the wind direction from predominantly a northwesterly direction to a northerly direction. This was due to the building of a high pressure system which moved in to dominate the whole of California subsequent to the passage of a frontal system early in the morning on 7 April 1978. There was no commensurate adjustment to meteorological parameters in the radiative transfer model.

Additional model calculations

In order to obtain some appreciation of the sensitivity of the radiative transfer model to the parameters used in the comparison calculations, some limited sensitivity computations are presented. The

TABLE 4 4/9/78: Comparison of Observed with Estimated Surface Flux (LY/min)

Hour	Surface Observation Locations 1	2	Avg	GOES Estimates	Ratio
08	0.622	0.603	0.61	0.63	1.03
10	1.140	1.130	1.12	1.14	1.02
12	1.326	1.312	1.32	1.35	1.02
13	1.282	1.275	1.28	1.31	1.02
14	1.166	1.216	1.19	1.18	0.99
15	0.969	0.968	0.97	0.98	1.01
16	0.687	0.778	0.73	0.71	0.97
Total integrated flux	131	132	131	133	1.02

variation of total incoming solar flux as a function of zenith angle of the sun is presented in Fig. 5. The calculations were made with a ground reflectivity of 0.25. The flux varies by a factor of three from a zenith angle of 0–70°. The average maximum flux difference between the cloud models (model C and model D1) is of the order of 25%. This difference is reduced to 10% for the cloud models. The calculated fluxes using the cloud models are approximately 33% less than those when the noncloud models are used. The incoming solar flux decreases rapidly as a function of zenith angle of the sun. This is primarily due to the rapid attenuation of the direct beam. The small, but significant, decrease in flux observed between model C and model Cl is due to the presence in model Cl of a slightly absorbing aerosol. The same phenomenon is also seen when comparing model D and model

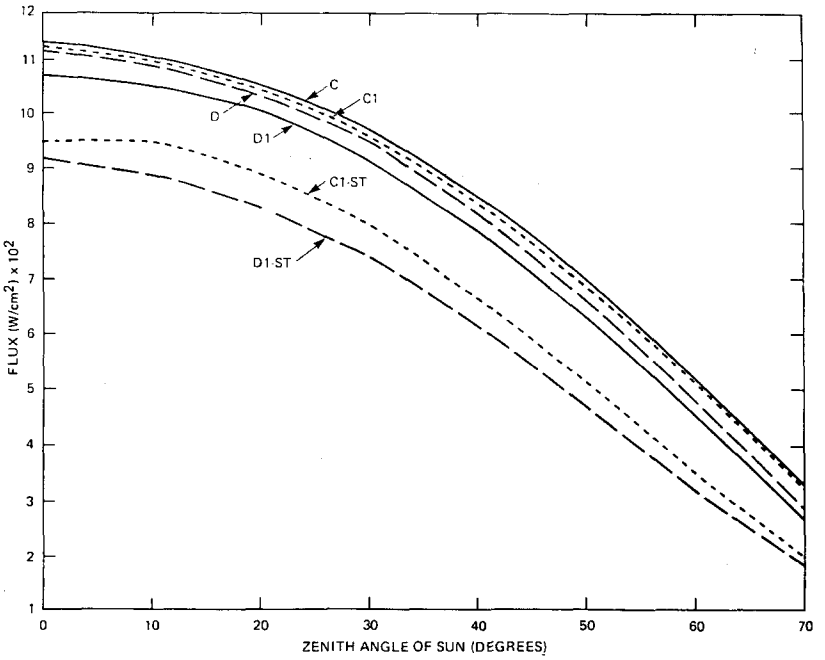

FIGURE 5. Computed surface total incoming flux as a function of local zenith angle of the sun for various atmospheric models for a Lambert surface reflectivity of 0.25.

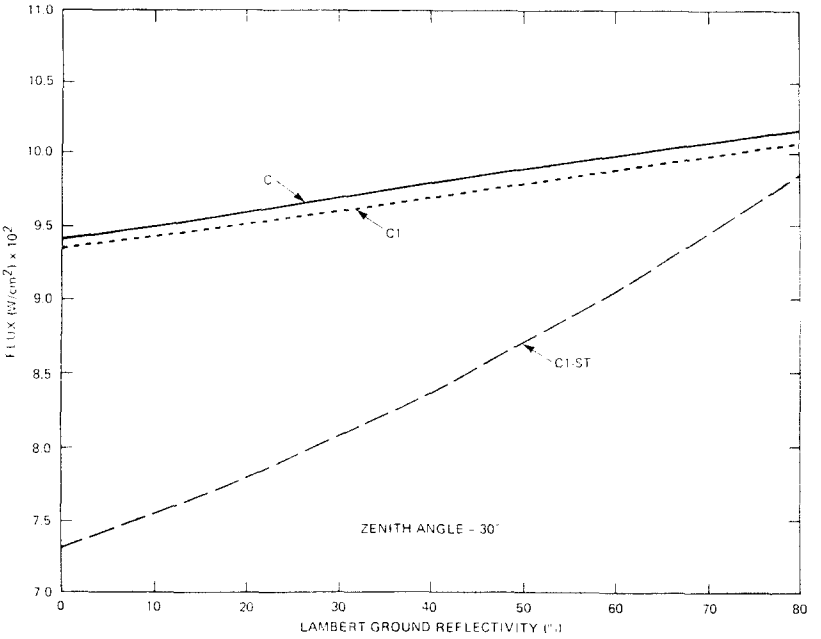

FIGURE 6(a). Computed surface total incoming flux as a function of Lambert ground reflectivity for the atmospheric models used in the comparison study (zenith angle = 30 °).

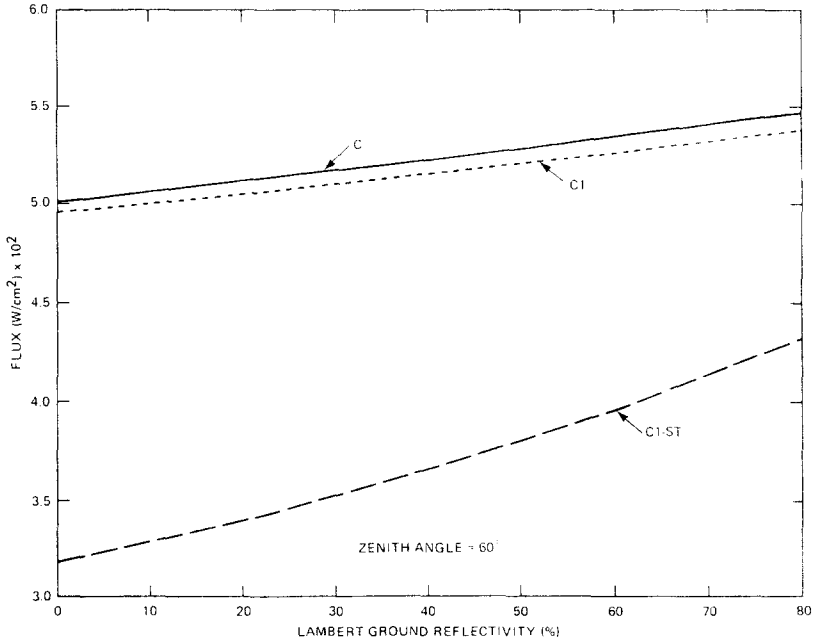

FIGURE 6(b). Computed surface total incoming flux as a function of Lambert ground reflectivity for the atmospheric models used in the comparison study (zenith angle = 60 °).

Dl. Figure 6(a) shows the variations of the flux as a function of ground reflectivity at a zenith angle of 30° for three models used in this study. The ground level flux for the noncloud models varies over the range of reflectivities by approximately 7%. The differences between the fluxes decrease as the ground reflectivity increases. The rate of change of the flux for the model C1-ST is much greater than for the no-cloud models. Therefore, a smaller change in ground reflectivity will cause a greater change in the flux when the cloud model is used than when the noncloud models are used. The effect on the variation of the flux of an increase in zenith angle to 60° is shown in Fig. 6(b). At this low sun position the noncloud models show a slightly greater reflectivity than at 30°. However, the cloud model C1-ST shows a decided reduced variation when compared to a zenith angle of 30°. Thus, it would appear that the model C1-ST is more sensitive to a change in ground reflectivity than the noncloud models. Furthermore, this sensitivity is highly dependent on zenith angle of the sun.

Concluding Remarks

We have presented a method of estimating ground-level solar insolation using observations from the GOES satellite and a radiative transfer model. The result of these computations when compared to surface observations under various sky conditions are within acceptable limits for many applications. A significant problem with the general use of the GOES digital values is the lack of an accurate and well-established conversion from digital values to intensities. Because of this, we had to rely on a first-order approximation approach for obtaining intensities from GOES digital values.

Ideally a technique for obtaining ground level solar flux should use satellite data to estimate the local area albedo. This would permit that initial estimates of albedo obtained under clear sky conditions can be used for cloudy conditions to estimate cloud amount. However, such a procedure must be first tested during a period and at a site for which both the albedo and cloud amounts are established. In the experiments described above, we tested our radiative model using surface albedo measurements to remove the uncertainty of this parameter from the method.

A major difficulty with the current one-dimensional radiative transfer model remains its use under less than total overcast conditions. The current method requires an estimate of sky cover and cloud type which is not always readily available. The transfer model also requires an estimate of the ground reflectivity. While the sensitivity of the surface simulated insolation to this parameter varies considerably for cloud models, its effect when a noncloud model is used is considerably reduced.

From an operational point of view, precalculated fluxes obtained by a sophisticated radiative transfer model and stored in a data set is very appealing. Specific atmospheric models could be added to the data set as required. These models would take into account local climatological parameters such as water vapor concentration and ozone amount. Local geological conditions as a function of ground reflectivity and aerosol type, amount, and vertical distribution could also be considered.

In the past, few potential users of solar flux data have had the computer resources for making complex radiative transfer calculations. But this is rapidly

changing with the advent of the microcomputer. These powerful and cost-efficient processors are putting computational tools in the hands of users who primarily had little or no access to computer facilities. Thus, simpler methods, currently being used because of lack of computer power now can be compared to more sophisticated radiative transfer models. We hopefully plan to carry out these comparisons.

The author wishes to express his gratitude to Mr. C. Staton of National Weather Service for his help in supplying GOES tapes for intensity calculations. The author wishes to thank Dr. J. L. Hatfield of the University of California-Davis for his assistance in supplying the surface data set. The author wishes to thank his colleagues Mr. N. S. Gussin for his valuable assistance in processing and archiving GOES tapes and Dr. J. V. Dave, who sparked the initial idea for this work.

References

Chen, E., Allen, L. H. Jr., Bartholic, J. F., Bill, R. G., Jr., and Sutherland, R. A. (1979), Satellite-sensed winter nocturnal temperature patterns of the Everglades agricultural area, *J. Appl. Meteorol.* 18: 992–1002.

Comeyne, G. J. (1980), Personal Communication, National Environmental Satellite Services, Washington, D.C.

Curran, R. J., and Man-Li, C. Wu (1982), Skylab near infrared observations of clouds indicating supercooled liquid water droplets, *J. Appl. Meteorol.* 39: 635–647.

Dave, J. V., and Braslau, N. (1975), Effect of cloudiness on the transfer of solar energy through radiative model atmosphere, *J. Appl. Meteorol.* 14: 388–395.

Davis, J. M., and Cox, S. K. (1982), Reflected solar radiances and regional scale scenes, *J. Appl. Meteorol.* 21: 1698–1712.

Deirmendjian, D. (1969), *Electromagnetic Scattering on Spherical Polydispersions*, Elsevier, New York, p. 290.

Gautier, C., Diak, G., and Masse, S. (1980), A simple physical model to estimate incident solar radiation at the surface from GOES satellite data, *J. Appl. Meteorol.* 19: 9–16.

Halpern, P., and Coulson, K. L. (1978), Solar radiative heating in the presence of aerosols, *IMB J. Res. Dev.* 22: 122–133.

Hanson, Kirby J. (1971), Studies of cloud and satellite parameterization of solar radiation at the earth's surface, Proceedings Miami Workshop on Remote Sensing, U.S. Department of Commerce, Miami, Florida, pp. 133–148.

McClatchey, R. A., Fenn, R. W., Selby, J. E. A., Garing, J. S., and Volz, F. E. (1970), Optical properties of the atmosphere, AFCRL-70-0527, Air Force Cambridge Research Laboratories, Bedford, Massachusetts.

Norton, C. C., Mosher, F. R., Hinton, B., Martin, D. W., Santek, D., and Kuhlow, W. (1980), A model for calculating desert aerosol turbidity over the oceans from geostationary satellite data, *J. Appl. Meteorol.* 19: 633–644.

Peterson, J. T., and Flowers, E. C. (1974), Urban–rural solar radiation and aerosol measurements in St. Louis and Los Angeles, Symposium on Atmospheric Diffusion and Air Pollution, Santa Barbara, California, pp. 129–141.

Reginato, R. J., Millard, J. P., Hatfield, J. L., and Jackson, R. D. (1981), Multilevel measurements of surface temperature over undulating terrain planted to barley, Final Report Contract No. S0255B NASA/ Goddard Space Flight Center, Greenbelt, Maryland.

Tarpley, J. D. (1979), Estimating incident solar radiation at the surface from geostationary satellite data, *J. Appl. Meteorol.* 18: 1172–1181.

Vonder Haar, T. H., and Ellis, J. S. (1975), Solar energy microclimate as determined from satellite observations, *Proc. Soc. Photo. Opt. Instrum. Eng.* 68: 18–22.

Received 19 May 1983; revised 19 August 1983.